An Energetically Feasible Mechanism for the Activation of the C−H Bond by the 16-Electron $CpM(PH_3)(CH_3)^+$ (M = Rh, Ir) Complex. A Theoretical Study

Ming-Der Su* and San-Yan Chu*

Contribution from the Department of Chemistry, National Tsing Hua University, Hsinchu 30043, Taiwan, ROC

Received June 3, 1996. Revised Manuscript Received March 24, 1997[⊗]

Abstract: The reaction mechanism for the activation of C−H bonds by coordinatively unsaturated $CpM(PH_3)(CH_3)^+$ (Cp = cyclopentadienyl; M = Rh, Ir) has been investigated by ab initio molecular orbital methods. Of the two possible mechanisms, an oxidative addition−reductive elimination process (path 1) and a σ-bond metathesis mechanism through a four-center transition state (path 2), only the former is found for the 16-electron Ir cation, while the Rh case might adopt the latter. The reaction trajectory of path 1 for the approach of $CpM(PH_3)(CH_3)^+$ to methane and the transition state structure can be predicted on the basis of a frontier molecular orbital model that determines the orientation of attack of the $CpM(PH_3)(CH_3)^+$ fragment on a doubly occupied canonical fragment molecular orbital of methane. From which, four kinds of reaction paths (paths A, B, C, and D) can be deduced due to the asymmetric nature of $CpM(PH_3)(CH_3)^+$. Both MP2 and QCISD results suggest that path A, where the methane C−H bond breaks on the ancillary CH_3 ligand side, is more favorable than other reaction paths kinetically and thermodynamically for both Rh and Ir cases. The calculational results strongly indicate that the reaction of the rhodium complex is intrinsically more difficult than that of the iridium complex. A qualitative model that is based on the theory of Pross and Shaik has been used to develop an explanation for the origin of the barrier height as well as the reaction enthalpy.

I. Introduction

The activation of carbon−hydrogen bonds by homogeneous transition-metal complexes is a topic that has increasingly received a great deal of attention.[1] Recently Bergman and Arndtsen reported that a cationic iridium complex $Cp^*(P(CH_3)_3)Ir(CH_3)(ClCH_2Cl)^+BAr_f^-$ [$Cp^* = \eta^5$-$C_5(CH_3)_5$; $BAr_f = B(3,5\text{-}C_6H_3(CF_3)_2)_4$] can thermally activate the carbon−hydrogen bond of methane as well as that of terminal alkanes in solution under milder conditions (10 °C) than in any previous works[2] (see Scheme 1). They believe that the high activity of such a complex **1** is undoubtedly due to the lability of the CH_2Cl_2 ligand, whose dissociation allows low-temperature access to the 16-electron fragment **2**, from which the reaction presumably undergoes either an oxidative addition−reductive elimination reaction (path 1) or a concerted 4-center transition state (path 2) for the C−H activation step. Of these two processes, it is well established that path 1 can be recognized,

Scheme 1

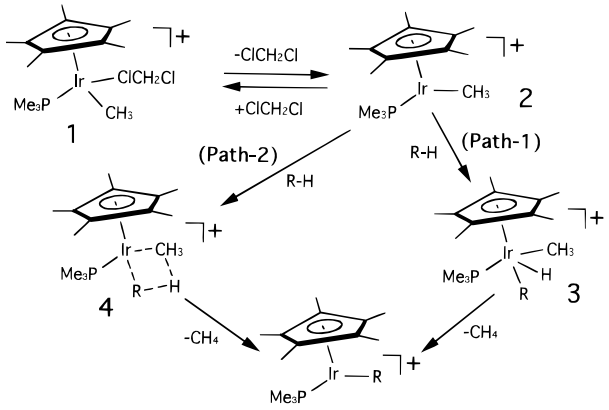

as it typically occurs with *late* transition metals, as an oxidative addition of a C−H bond to a metal center to form a (hydrido)-(alkyl) metal complex (such as **3** in Scheme 1) via a three-center transition state.[3] On the other hand, path 2 is generally referred to as σ-bond metathesis, since the alkane C−H bond adds a bond to an electropositive metal (usually an *early* metal, i.e., f-element) via a four-center transition state, leading to a new metal alkyl complex (such as **4** in Scheme 1).[4]

This aroused our interest to investigate the potential energy surfaces of the $CpM(PH_3)(CH_3)^+ + CH_4$ (Cp = η^5-C_5H_5; M = Ir, Rh) model system using the ab initio molecular orbital methods.[5] Our aim is to search for the energetically feasible

[⊗] Abstract published in *Advance ACS Abstracts,* May 15, 1997.

(1) For reviews, see: (a) Parshall, G. W. *Acc. Chem. Res.* **1975**, *8*, 113. (b) Bergman, R. G. *Science* **1984**, *223*, 902. (c) Janowicz, A. H.; Perima, R. A.; Buchanan, J. M.; Kovac, C. A.; Struker, J. M.; Wax, M. J.; Bergman, R. G. *Pure Appl. Chem.* **1984**, *56*, 13. (d) Hill, C. L. *Activation and Functionalization of Alkanes*; Wiley: New York, 1989. (e) Halpern, J. *Inorg. Chim. Acta* **1985**, *100*, 41. (f) Ephritikhine, M. *New J. Chem.* **1986**, *10*, 9. (g) Jones, W. D.; Feher, F. J. *Acc. Chem. Res.* **1989**, *22*, 91. (h) Ryabov, A. D. *Chem. Rev.* **1990**, *90*, 403. (i) Davies, J. A.; Watson, P. L.; Liebman, J. F.; Greenberg, A. *Selective Hydrocarbon Activation, Principles and Progress*; VCH Publishers. Inc.: New York, 1990. (j) Bergman, R. G. *J. Organomet. Chem.* **1990**, *400*, 273. (k) Koga, N.; Morokuma, K. *Chem. Rev.* **1991**, *91*, 823. (l) Ziegler, T. *Chem. Rev.* **1991**, *91*, 651. (m) Bergman, R. G. *Adv. Chem. Ser.* **1992**, *230*, 211. (n) Wasserman, E. P.; Moore, C. B.; Bergman, R. G. *Science* **1992**, *255*, 315. (o) Crabtree, R. H. *Angew. Chem., Int. Ed. Engl.* **1993**, *32*, 789. (p) Schroder, D.; Schwarz, H. *Angew. Chem., Int. Ed. Engl.* **1995**, *34*, 1937. (q) Lees, A. J.; Purwoko, A. A. *Coord. Chem. Rev.* **1994**, *132*, 155. (r) Amdtsen, B. A.; Bergman, R. G.; Mobley, T. A.; Peterson, T. H. *Acc. Chem. Res.* **1995**, *28*, 154. (s) Ziegler, T. *Can. J. Chem.* **1995**, *73*, 743.

(2) (a) Arndtsen, B. A.; Bergman, R. G. *Science* **1995**, *270*, 1970 and references therein. (b) Lohrenz, J. C.; Jacobsen, H. *Angew. Chem., Int. Ed. Engl.* **1996**, *35*, 1305.

(3) (a) Janowicz, A. H.; Bergman, R. G. *J. Am. Chem. Soc.* **1983**, *105*, 3929. (b) Bergman, R. G. *Science* **1984**, *223*, 902. (c) Jones, W. D.; Feher, F. J. *J. Am. Chem. Soc.* **1984**, *106*, 1650.

(4) (a) Watsen, P. L. *J. Am. Chem. Soc.* **1983**, *105*, 6491. (b) Watsen, P. L.; Parshall, G. W. *Acc. Chem. Res.* **1985**, *18*, 51. (c) Fendrick, C. M.; Marks, T. J. *J. Am. Chem. Soc.* **1984**, *106*, 425.

(5) An excellent and short paper was published when this manuscript was submitted. Strout, D. L.; Zaric, S.; Niu, S.; Hall, M. B. *J. Am. Chem. Soc.* **1996**, *118*, 6068.

S0002-7863(96)01847-1 CCC: $14.00

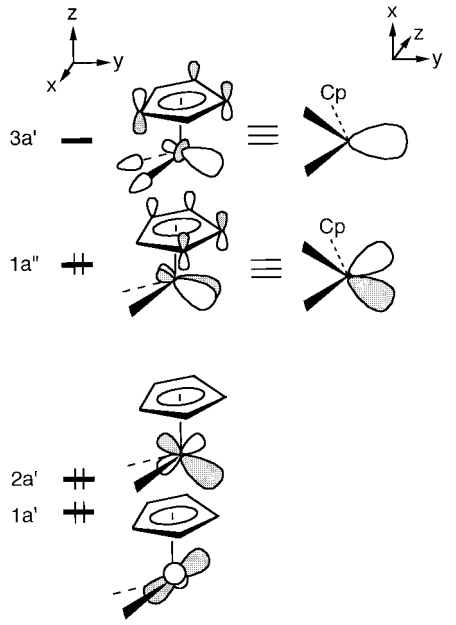

Figure 1. A frontier orbital diagram for 16-electron $CpM(CO)_2$.

reaction pathway for such reactions, and to bring out the determined factor that controls the activation barrier for the oxidative addition of the $CpM(PH_3)(CH_3)^+$ complexes. It will be shown that the singlet−triplet gap of the $CpM(PH_3)(CH_3)^+$ (M = Rh, Ir) species can be a guide to predict its reactivity for oxidative addition reactions.

II. The Electronic Structure of $CpM(PH_3)(CH_3)^+ + CH_4$

The major purpose in this section is to outline the electronic details of the bonding for 16-electron $CpM(PH_3)(CH_3)^+ + CH_4$ systems, focusing on the issue: What sort of interactions do exist between orbitals of 16-electron $CpM(PH_3)(CH_3)^+$ and those of methane? One may then build up a frontier molecular orbital (FMO) model, based on a set of fragment MOs, which has been proved to be a good approach that allows one to predict the approximate reaction trajectory and transition state structure for the insertion of the electrophile into the saturated C−H bonds, such as an oxygen atom insertion[6a] and carbene insertion[6b] reactions. It has to be mentioned that this concept of insertion mechanism was expressed for the first time by Bach.[6] In the present work, we shall therefore use the FMO model to search for the transition states of the oxidative addition reaction of the $CpM(PH_3)(CH_3)^+$ complex that is isolobal to methylene as well as the oxygen atom (*vide infra*).[7]

We first consider the electronic structures of the 16-electron $CpM(PH_3)(CH_3)^+$ fragment. Although the $CpM(PH_3)(CH_3)^+$ complex contains asymmetric ligands, the MOs of such an asymmetric fragment can easily be related to those of the symmetric $CpM(CO)_2$ fragment. A general outline of the frontier orbitals in $CpM(CO)_2$, which are explicitly shown in Figure 1, has been extensively studied.[8] In the 16-electron case, the frontier orbitals for $CpM(CO)_2$ consist of three occupied levels, 1a′, 2a′, and 1a″, under C_s symmetry, which are primarily made up of transition metal d orbitals, i.e., $x^2 - y^2$, *yz*, and *xz*. In the higher vacant level (3a′), d_z^2 is hybridized with s and p_z character in such a way that the orbital lobes point away from the ancillary ligands. When the symmetry is broken, the character of these orbitals changes, and the introduction of different ligands with varying donor and acceptor capabilities may affect the position of the energy levels. Nevertheless, according to the theoretical analysis based on the method we used in this work, it was found that such an intramolecular perturbation does not affect the relative positions of the energy levels of the frontier orbitals. Namely, the highest occupied MO (HOMO) and the lowest unoccupied MO (LUMO) for the asymmetric 16-electron $CpM(PH_3)(CH_3)^+$ fragment are still 1a″ and 3a′, respectively.

Moreover, in a canonical MO description of a hydrocarbon, there are no isolated MOs that describe a particular C−H σ bond. For example, in methane there is a lower lying $2A_1$ orbital and three degenerate T_2 orbitals.[9] In a tetrahedral array, both hydrogens (or carbons) directly bound to the sp^3 carbon occupy a common plane, and they are related by symmetry and may comprise an orbital with σ symmetry (σ_{CH2}) as in **5** or a π_{CH2} orbital as in **6**.[10]

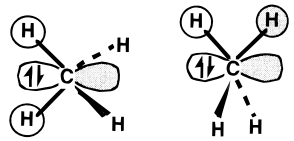

σ_{CH2} π_{CH2}

5 **6**

As mentioned earlier, since 16-electron $CpM(PH_3)(CH_3)^+$ and CH_2 are isolobal,[7] then each should have two valence orbitals with the same symmetry properties. These are shown in **7**, in which each fragment has one orbital of a′ and a″ symmetry.

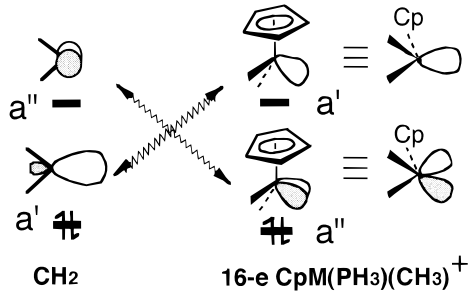

7

Note that the energy ordering in the metal fragment differs from that in the carbene. This is a natural consequence of the fact that in $CpM(PH_3)(CH_3)^+$ the major contribution to the a″ orbital is the metal d character, while in the a′ orbital it is a hybrid of metal s, p, and d character (*vide supra*). Therefore, for a singlet CH_2 fragment, one would assign the two electrons to the a′ orbital, while for a singlet 16-electron $CpM(PH_3)(CH_3)^+$ species, the two electrons would go into the a″ level. In other words, the frontier orbitals of the 16-electron $CpM(PH_3)(CH_3)^+$

(6) (a) Bach, R. D.; Andres, J. L.; Su, M.-D.; McDouall, J. J. W. *J. Am. Chem. Soc.* **1993**, *115*, 5768. (b) Bach, R. D.; Su, M.-D.; Aldabagh, E.; Andres, J. L.; Schlegel, H. B. *J. Am. Chem. Soc.* **1993**, *115*, 10237. (c) Bach, R. D.; Su, M.-D. *J. Am. Chem. Soc.* **1994**, *116*, 10103.

(7) Hoffmann, R. *Angew. Chem., Int. Ed. Engl.* **1982**, *21*, 711.

(8) (a) Hoffmann, P. *Angew. Chem.* **1977**, *89*, 551. (b) Schilling, B. E. R.; Hoffmann, R.; Lichtenberger, D. L. *J. Am. Chem. Soc.* **1979**, *101*, 585. (c) Schilling, B. E. R.; Hoffmann, R.; Faller, J. W. *J. Am. Chem. Soc.* **1979**, *101*, 592.

(9) (a) For a discussion, see: Jorgensen, W. L.; Salem, L. *The Organic Chemist's Book of Orbitals*; Academic Press: New York, 1973. (b) Meredith, C.; Hamilton, T. P.; Schaefer, H. F., III *J. Phys. Chem.* **1992**, *96*, 9250.

(10) In this work, we shall use the σ/π nomenclature (see ref 6) to describe the reaction trajectory and define the axis of attack of the valence orbital on the central metal.

complex consist of an empty s/p/d hybrid orbital and a d orbital that has a single lone pair of electrons. It is noteworthy that in the latter orbital (a″), the d lobe points along the basal direction, if $CpML_2$ is considered to be a pseudo-square-pyramid molecule.

Therefore, we prefer to use a canonical MO rather than take a localized description of the C−H bond, since it is easier to visualize the coalescence of the electron donor and acceptor when the approximate axis of the reaction is clearly defined. In this qualitative theoretical treatment, we identify the organotransition-metal fragment $CpM(PH_3)(CH_3)^+$ as having an empty electrophilic orbital (i.e., 3a′ as shown in Figure 1 or **7**) that can interact with either the doubly occupied σ_{CH_2} (**5**) or the doubly occupied π_{CH_2} (**6**) fragment orbital in methane to arrive at a saddle point. In other words, as illustrated in Figure 2, the FMO model suggests that the the starting geometry of 16-electron $CpM(PH_3)(CH_3)^+$ may approach methane from two unique directions. For the σ-attack, the 3a′ orbital of $CpM(PH_3)(CH_3)^+$ overlaps with a hydrocarbon fragment along the axis of its filled atomic p orbital and a 1,2-hydrogen migration to the adjacent pair of electrons (1a″) takes place in concert with the C−M bond formation. On the other hand, the π-attack proceeds by attack of a filled π_{CH_2} fragment orbital along the axis of the empty s/p/d orbital of $CpM(PH_3)(CH_3)^+$ with a concerted hydrogen migration into the $CpM(PH_3)(CH_3)^+$ lone pair. As a result, the net molecular event involved in the insertion of the $CpM(PH_3)(CH_3)^+$ complex into a C−H σ bond of methane is the formation of a new metal−carbon σ bond as well as a new metal−hydrogen σ bond, accompanied by the breaking of the C−H σ bond. This is a typical example for the oxidative addition reaction of a transition metal complex into the C−H bond.[1] We shall see the calculational results supporting these predictions below.

III. Computational Methods

Ab initio molecular orbital calculations were performed with the GAUSSIAN 94 program.[11] The geometries of the investigated species were fully optimized without imposing any symmetry constraints, by gradient-based techniques,[12] at the Møller−Plesset level of theory[13] truncated at second order (MP2(FULL)). For triplet $CpM(PH_3)(CH_3)^+$ systems, we also carried out the second-order unrestricted MP calculations (UMP2) with annihilation of the spin contaminants (PUMP2).[14]

Effective core potentials (ECP) were used to represent the 28 and 60 innermost electrons of the rhodium (up to the 3d shell) and iridium (up to the 4f shell) atoms,[15] respectively, as well as the 10-electron core of the phosphorus atom.[16] For these atoms, the basis set was that associated with the pseudopotential,[15,16] with a standard LANL2DZ contraction.[11] For hydrogens and carbon atoms the double-ζ basis of Dunning−Huzinaga was used.[17] Thus, the model compound $CpM(PH_3)(CH_3)^+ \cdot CH_4$ (M = Rh, Ir) has 123 basis functions and 78 electrons. The MP2 calculation was therefore denoted by MP2/LANL2DZ. Vibrational frequencies at stationary points were calculated at the MP2/LANL2DZ level of theory to identify them as minima (zero imaginary frequencies) or transition states (one imaginary frequency).

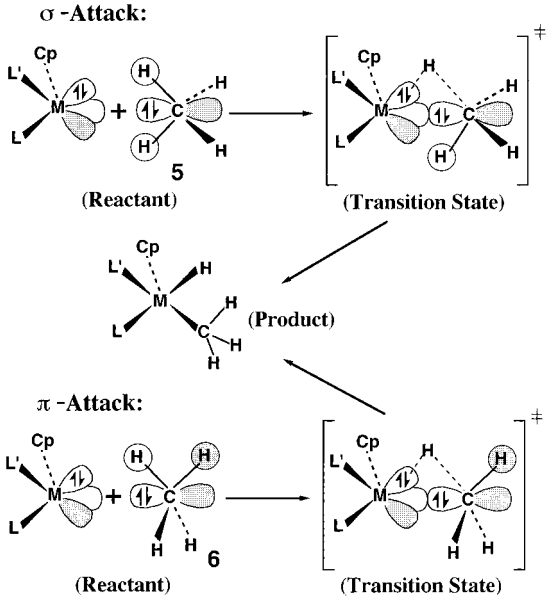

Figure 2. The insertion of 16-electron $CpM(L)(L')^+$ (L, L′ = PH_3, CH_3) into hydrocarbons can proceed along a σ_{CH_2} path, where the empty $CpM(L)(L')^+$ s/p/d orbital is aligned with the carbon p orbital of a σ_{CH_2} fragment orbital, or along a π_{CH_2} path, where the $CpM(L)(L')^+$ s/p/d orbital is aligned with a π_{CH_2} fragment orbital.

As suggested by one referee, to better evaluate the relative stability of the investigated species, several single-point calculations were performed at the MP2/LANL2DZ optimized geometries, by quadratic configuration interaction theory,[18] including the contributions from single and double excitations (QCISD).

IV. Results and Discussion

1. The Potential Energy Surfaces of $CpIr(PH_3)(CH_3)^+$. We first discuss the calculational results of the $CpIr(PH_3)(CH_3)^+$ model system. It must be mentioned that, for σ-attack, one can consider two paths of methane approach depicted in **8**. In path

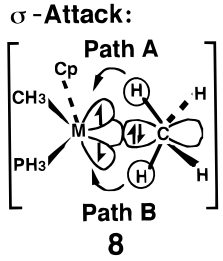

A, the methane C−H bond breaks on the ancillary CH_3 ligand side, whereas in path B, the methane C−H bond cleaves on the ancillary PH_3 ligand side. Likewise, for π−attack, two similar pathways (path C, **9**, and Path D, **10**) may occur for the methane C−H bond breaking on the CH_3 ligand side and the PH_3 ligand side, respectively. Thus, we utilized the MP2/LANL2DZ level of theory for geometry optimization for the above four reaction paths, whose stationary point structures thus obtained are shown in Figures 3 and 4, respectively. No experimental geometries are available for them. Their energy parameters at the MP2/LANL2DZ and QCISD//MP2/LANL2DZ levels are collected in Table 1.

Several interesting results can be drawn from Figures 3 and 4 and Table 1. First, as seen from Table 1, the QCISD results indicate that the ground state of the 16-electron $CpIr(PH_3)(CH_3)^+$ species should be singlet. The first triplet state lies 17

(11) Gaussian 94, Revision B.2: M. J. Frisch, G. W. Trucks, H. B. Schlegel, P. M. W. Gill, B. G. Johnson, M. A. Robb, J. R. Cheeseman, T. Keith, G. A. Petersson, J. A. Montgomery, K. Raghavachari, M. A. Al-Laham, V. G. Zakrzewski, J. V. Ortiz, J. B. Foresman, J. Cioslowski, B. B. Stefanov, A. Nanayakkara, M. Challacombe, C. Y. Peng, P. Y. Ayala, W. Chen, M. W. Wong, J. L. Andres, E. S. Replogle, R. Gomperts, R. L. Martin, D. J. Fox, J. S. Binkley, D. J. Defrees, J. Baker, J. P. Stewart, M. Head-Gordon, C. Gonzalez, and J. A. Pople; Gaussian, Inc.: Pittsburgh, PA, 1995.

(12) Schlegel, H. B. *J. Comput. Chem.* **1982**, *3*, 214.

(13) Møller, C.; Plesset, M. S. *Phys. Rev.* **1934**, *46*, 618.

(14) Sosa, C.; Schlegel, H. B. *J. Am. Chem. Soc.* **1987**, *109*, (a) 4193, (b) 7007.

(15) Hay, J. P.; Wadt, W. R. *J. Chem. Phys.* **1985**, *82*, 299.

(16) Hay, J. P.; Wadt, W. R. *J. Chem. Phys.* **1985**, *82*, 284.

(17) Dunning, T. H.; Hay, P. J. *Modern Theoretical Chemistry*; Schaefer, H. F., Ed.; Plenum: New York, 1976; pp 1−28.

(18) Pople, J. A.; Head-Gordon, M.; Raghavachari, K. J. *J. Chem. Phys.* **1987**, *87*, 5968.

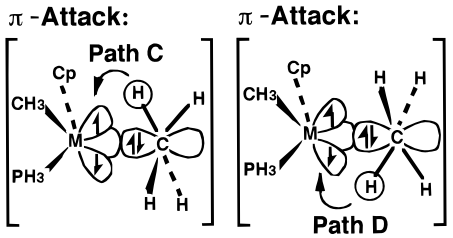

9 **10**

kcal/mol above. Thus, it is reasonable to predict that the whole reaction for the $CpIr(PH_3)(CH_3)^+$ system will adopt a singlet process without the participation of the diradical intermediates. Additionally, as shown in Figures 3 and 4, the distance Ir−X between the iridium atom and the center, X, of the Cp ring and the distances M−L and M−L′ are larger for the triplet compared with the singlet. This is a result of single occupancy of the 3a′ orbital in the triplet state, which has M−Cp, M−L, and M−L′ antibonding character as depicted in Figure 1.

Second, our calculations suggest that the agostic complex (**Ir-Cpx-A**) for the $CpIr(PH_3)(CH_3)^+ + CH_4$ reaction may be observable in the reaction with a stabilization energy of about 10 kcal/mol at the MP2 level and 7.1 kcal/mol at the QCISD level. In addition, checking the geometrical structures of the agostic complexes (**Ir-Cpx-A**, **Ir-Cpx-B**, **Ir-Cpx-C**, and, **Ir-Cpx-D**) for each path in Figures 3 and 4, it appears that, in principle, methane may bind side-on through a single C−H σ-bond, i.e., in a η^2-C,H fashion. Moreover, as seen in Figures 3 and 4, the distance between carbon and the migrating hydrogen in the methane moiety for the agostic complexes studied here is slightly elongated (1.15−1.16 Å).

Third, four kinds of transition state were found for the $CpIr(PH_3)(CH_3)^+ + CH_4$ reaction: **Ir-TS-A**, **Ir-TS-B** (Figures 3), **Ir-TS-C**, and **Ir-TS-D** (Figures 4). One of the basic tenets of the FMO theory shown in Figure 2 is that insertion of an organometallic reagent into a C−H bond involves the entire CH_2 fragment orbital and not just an isolated C−H σ-bonding orbital. Examination of the single imaginary frequency for oxidative additions of methane provides excellent confirmation of this concept where $CpIr(PH_3)(CH_3)^+$ attacks either the σ_{CH_2} or π_{CH_2} fragment orbital along the axis of the carbon 2p orbital. Animation of these imaginary frequencies clearly shows a rocking motion of the entire either σ_{CH_2} or π_{CH_2} fragment (H_1−C−H_2) as indicated by the vectors on both H_1 and H_2 (see the heavy arrows in Figures 3 and 4). In addition, it is evident that these transition vectors all are in accordance with the insertion process, primarily the C−H bond stretching with a hydrogen migrating to the metal center. In other words, those transition states proceed in a three-center pattern involving the metal center and carbon and hydrogen atoms undergoing bond cleavage. Note that such characteristic three-centered cyclic transition states are consistent with mechanisms for oxidative additions of 16-electron CpML systems, postulated by Bergman et al.[3a,b] and Jones et al.[3c,19] Furthermore, it must be emphasized that, for the Ir case, all attempts to find any transition state with a four-center pattern (path 2 in Scheme 1) led directly to the three-center fashion (path 1 in Scheme 1), and it is certain that the four-center transition state does not exist at the present level of theory. In fact, it is not surprising to have such a stereochemical consequence since the FMO model demonstrated in Figure 2 provides a solid basis for predicting the potential existence of the three-centered cyclic transition state.

(19) For a theoretical study of the oxidative additions of the 16-electron CpML systems using the FMO model presented in this work see: Su, M.-D.; Chu, S.-Y. *J. Phys. Chem.* In press.

Fourth, four kinds of intermediate (**Ir-Int-A**, **Ir-Int-B**, **Ir-Int-C**, and **Ir-Int-D**) which are deduced from the corresponding **Ir-TS-A**, **Ir-TS-B**, **Ir-TS-C**, and **Ir-TS-D**, respectively, were also found. See Figures 3 and 4. It must be pointed out that these four intermediates (i.e., local minima) are basically the oxidative addition products. The most striking difference among the four intermediates is, for instance, in **Ir-Int-A**, the migrating hydrogen atom (H_1) has an equal distance (2.24 Å) with the carbon atom (C_1) of the incoming methane as well as the carbon atom (C_2) of the ancillary CH_3 ligand. This may allow H_1 to couple readily with either C_1 or C_2 to form the C−H bond, and then the reductive elimination reaction easily proceeds: **Ir-Int-A** → **Ir-TS-A** → **Ir-Cpx-A** (*vide infra*). In contrast, the migrating hydrogen atom (H_1) of **Ir-Int-B** has an unequal distance with the carbon atom (C_1) of the incoming methane and the carbon atom (C_2) of the ancillary CH_3 ligand by 2.27 and 3.55 Å, respectively, which makes it difficult for the Ir complex to proceed in the reductive elimination in forming the C−H bond compared with path A. Similar results can also be found in **Ir-Int-C** and **Ir-Int-D**. Thus, from the stereochemical viewpoint, it appears that path A would be more appropriate for the reaction of $CpIr(PH_3)(CH_3)^+$ with methane than other reaction paths. Moreover, since the energy differences among the four transition states, as well as the four intermediates, are small and in a realistic system the ancillary PR_3 ligand has sterically bulky groups which should hinder the activation of the C−H bond, it is reasonable to conclude that the activation of the methane C−H bond will occur on the ancillary CH_3 ligand side, rather than on the ancillary PR_3 ligand side. On the other hand, one may anticipate that if the sterically bulky group attached on the C_2 atom instead of the P atom, then the methane C−H bond breaking will prefer to take place on the ancillary PH_3 ligand side due to the steric effect. This effect will, in turn, decrease the reaction efficiency and may perhaps stop its oxidative addition reaction to alkanes.

Fifth, as seen in Table 1, of the four paths, paths A and B are more favorable than paths C and D in energetics at the MP2 level of calculation, although the energy differences among them are small. Moreover, it is clear to see that at our highest level of theory, QCISD, the electron correlation effect does not change the energy difference between path A and path B significantly. For these reasons, we shall therefore concentrate on the calculational results of path A and path B at the QCISD level from now on; paths A and B potential energy profiles are summarized in Figure 5. It is noteworthy that, as shown in Figure 5, since the reactants and the products of the reaction are identical, the potential energy curves are symmetric with respect to midpoints (i.e., the intermediate) of the reaction coordinates.

Sixth, as given in Figure 5, the fact that the stabilization energy for the agostic complex (e.g., **Ir-Cpx-A** and **Ir-Cpx-B**, 7.1 kcal/mol) is larger than that for the intermediate (e.g., **Ir-Int-A**, 0.30 kcal/mol; **Ir-Int-B**, 1.3 kcal/mol) may point to the intriguing conclusion that the latter cannot be isolated experimentally. The reason that the agostic complexes are much more stable than the fully-bonded intermediates is presumably because the central metal (Ir) acts as a Lewis acid. Qualitatively, since oxidative addition involves charge transfer from the metal center of $CpML_2$ to the incoming methane, a charged $CpIr(PH_3)(CH_3)^+$ species implying the decrease of the electron density on the central metal would make its oxidative addition product (i.e., **Ir-Int-A** and **Ir-Int-B**) unstable and then lower the exothermicity. Furthermore, the QCISD results suggest that the energies of **Ir-TS-A** and **Ir-TS-B** are above the energy of the reactants by 5.4 and 6.0 kcal/mol, respectively, and the activation

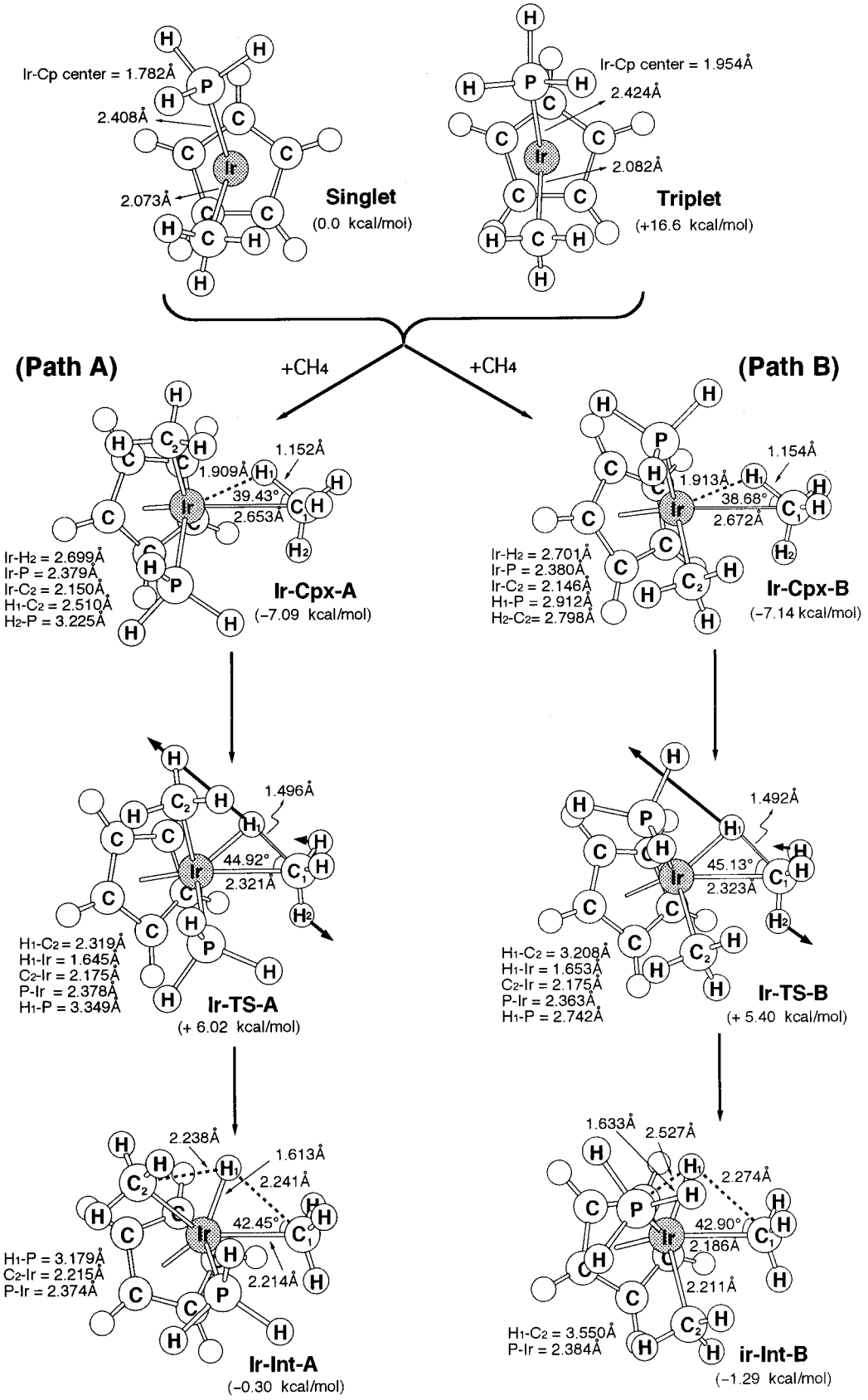

Figure 3. The MP2/LANL2DZ optimized geometries at reactants (singlet and triplet), agostic complexes (Cpx), transition states (TS), and intermediate (Int) of $CpIr(PH_3)(CH_3)^+$ for path A and path B. See the text for details. The numbers in parentheses are the relative energies at the QCISD//MP2/LANL2DZ level. The heavy arrows indicate transition vectors for the single imaginary frequency described by the transition states **Ir-TS-A** (−636 cm^{-1}) and **Ir-TS-B** (−649 cm^{-1}).

energy for the overall reaction is about 13 kcal/mol. It is in principle conceivable that when other effects (such as the solvent effect) are taken into account, this activation barrier will be greatly reduced. Though we have not carried out such a calculation, the present results indicate that the activation of the methane C−H bond by $CpIr(PH_3)(CH_3)^+$ should take place

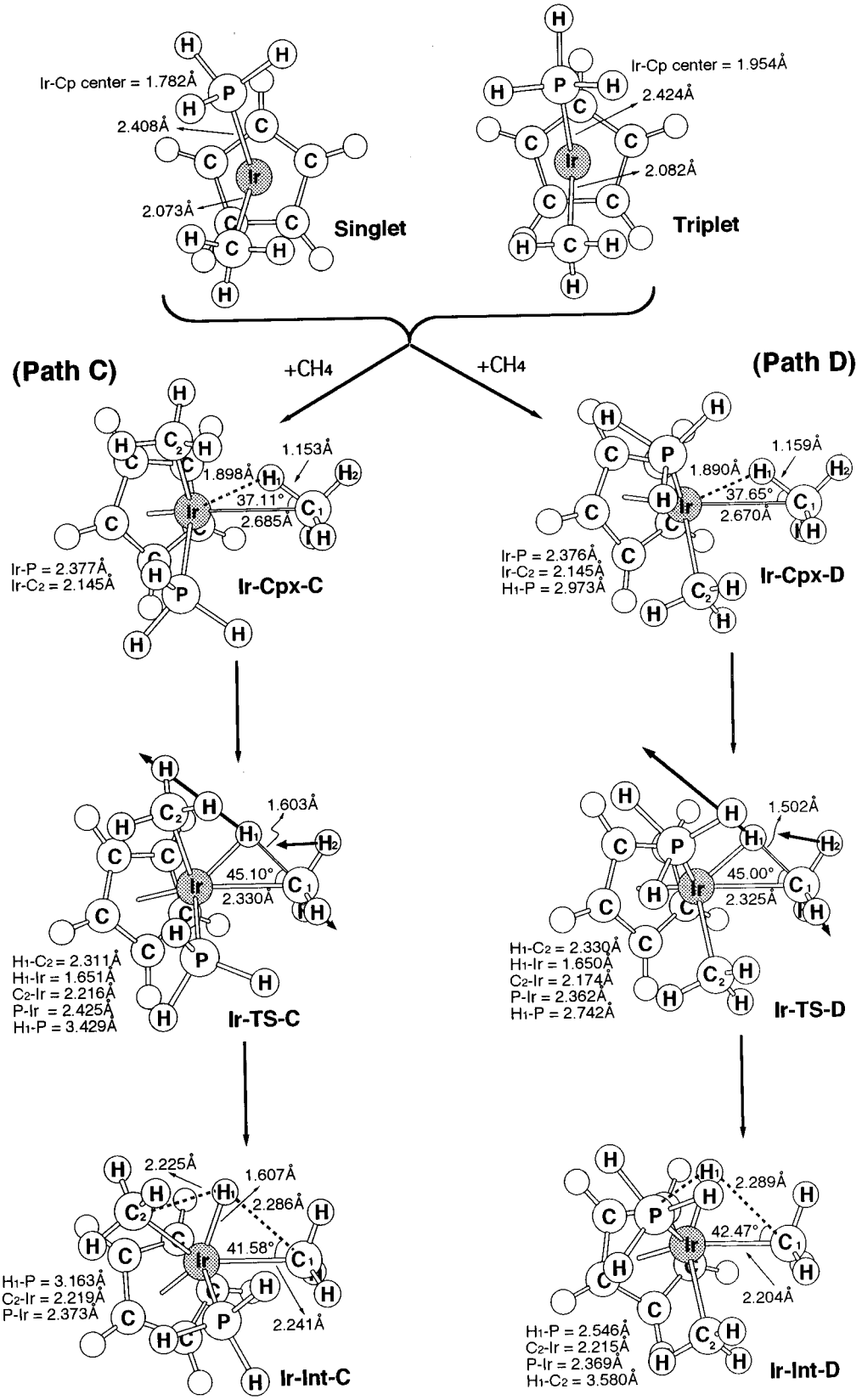

Figure 4. The MP2/LANL2DZ optimized geometries at reactants (singlet and triplet), agostic complexes (Cpx), transition states (TS), and intermediate (Int) of $CpIr(PH_3)(CH_3)^+$ for path C and path D. See the text for details. The heavy arrows indicate transition vectors for the single imaginary frequency described by the transition states **Ir-TS-C** (-611 cm^{-1}) and **Ir-TS-D** (-638 cm^{-1}).

easily, in agreement with the experimental findings.[2] Certainly, to obtain the more precise value for such a barrier height requires special computational studies as well as available experimental data. Such studies, however, are beyond the scope of the present work.

After this paper was submitted, an independent paper concerning the mechanism in the activation of methane by the iridium complex using density functional theory was published.[5] In that work, the same model system ($CpIr(PH_3)(CH_3)^+$) was used as we discussed in the present study. The results and conclusions based on the B3LYP/LANL2DZ level described in that paper are remarkably similar to those presented here.

Table 1. Relative Energies for Singlet and Triplet $CpM(PH_3)(CH_3)^+$ Fragments and for the Process CH_4 + $CpM(PH_3)(CH_3)^+$ → Agostic Complex (Cpx) → Transition State (TS) → Intermediate (Int) → Transition State (TS) → Agostic Complex (Cpx) → $CpM(PH_3)(CH_3)^+$ + CH_4[a]

	M = Ir		M = Rh	
	MP2[b]	QCISD[c]	MP2[b]	QCISD[c]
singlet	−344.17580	−344.22956	−349.00626	−349.05610
triplet[d]	+20.9	+16.6	+31.8	+20.4
Cpx-A[e]	−10.3	−7.09	−11.9	−9.50
Cpx-B	−10.2	−7.14	−11.6	−9.24
Cpx-C	−9.62		−10.9	
Cpx-D	−9.79		−10.7	
TS-A[e]	−2.51	+6.02	+7.95	+18.7
TS-B	−3.40	+5.40	+8.52	+19.9
TS-C	−1.21		+9.59	
TS-D	−3.08		+9.68	
Int-A[e]	−14.4	−0.300	+2.86	+21.0
Int-B	−16.1	−1.29	+1.82	+22.1
Int-C	−10.8		+5.62	
Int-D	−13.8		+4.17	

[a] For stationary point structures for Ir and Rh cases see Figures 3, 4 and Figures 6, 7, respectively. [b] At the MP2/LANL2DZ level; in hartrees. The energy of CH_4 at the MP2/LANL2DZ level is −40.27915 hartrees. [c] At the QCISD//MP2/LANL2DZ level; in hartrees. The energy of CH_4 at the QCISD//MP2/LANL2DZ level is −40.29845 hartrees. [d] The energy relative to the corresponding singlet state. [e] The energy relative to the corresponding singlet reactants.

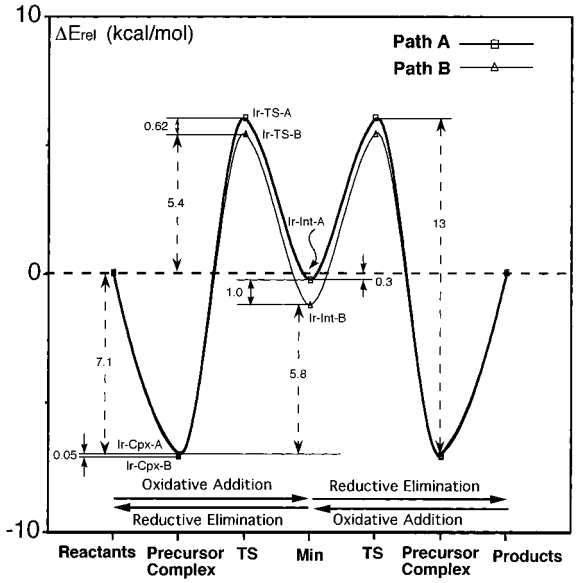

Figure 5. Potential energy surfaces for the activation of the methane C−H bond by $CpIr(PH_3)(CH_3)^+$. The relative energies are taken from the QCISD//MP2/LANL2DZ level as given in Table 1. The heavy solid curve indicates path A, while the solid curve indicates path B. For the MP2 optimized structures of the stationary points for paths A and B see Figure 3.

For instance, B3LYP calculations suggest that $CpIr(PH_3)(CH_3)^+$ must proceed through a three-center adduct and its barrier to methane metathesis is 11.5 kcal/mol. Nevertheless, the most conspicuous difference between B3LYP/LANL2DZ (in Hall *et al*.) and QCISD//MP2/LANL2DZ (in this work) has two points: first, the stabilization energy of the agostic structure in the former is 1.0 kcal/mol, while that in the latter is 7.0 kcal/mol; second, the energy of the intermediate in the former is above the energy of the reactants by 3.4 kcal/mol, whereas that in the latter is below the energy of the reactants by about 1.0 kcal/mol.

2. The Potential Energy Surfaces of $CpRh(PH_3)(CH_3)^+$. For comparison, we have also examined the mechanisms for the activation of the methane C−H bond by the isoelectronic $CpRh(PH_3)(CH_3)^+$ complex. Stationary point structures on paths A, B (**8**), C (**9**), and D (**10**) at the MP2/LANL2DZ level are shown in Figures 6 and 7, respectively. Their energy parameters at the MP2/LANL2DZ and QCISD//MP2/LANL2DZ levels are collected in Table 1.

Basically, the calculational results of $CpRh(PH_3)(CH_3)^+$ resemble those noted above for the $CpIr(PH_3)(CH_3)^+$ system in many aspects. For example, as seen in Table 1, we would expect the ground state of $CpRh(PH_3)(CH_3)^+$ to be a singlet (with the first triplet state lying 20 kcal/mol at the QCISD level of theory). Thus, it is reasonable to conclude that the 16-electron Rh cation will adopt a singlet process without the participation of the diradical intermediates. Again, for the rhodium case, both the σ_{CH_2} and π_{CH_2} approach depicted in Figure 2 can lead to a first-order saddle point, as determined by the frequency calculations at the MP2/LANL2DZ level. Their normal modes associated with the single imaginary frequency, as shown by the heavy arrows in Figures 6 and 7, are consistent with the C−H activation process, mainly C−H bond stretching and H transfer. Additionally, in MP2 energetics path A was found to be the most favorable in those four reaction paths, followed by path B. We therefore summarize the potential energy profiles of paths A and B at the QCISD//MP2/LANL2DZ level in Figure 8.

In comparison of Figure 8 with Figure 5, the most dramatic change occurs in the position of the intermediate (i.e., **Rh-Int-A** and **Rh-Int-B**) on the reaction paths, whose energy is apparently higher than the energy of the corresponding transition state (i.e., **Rh-TS-A** and **Rh-TS-B**, respectively) by 2−3 kcal/mol. Thus, our QCISD calculations might imply that the energy curve in Figure 8 could be interpreted as a σ-bond metathesis pathway with the so-called intermediate as the transition state. Moreover, the activation barrier for $CpRh(PH_3)(CH_3)^+$ was calculated to be 28 kcal/mol, which is twice as large as that for $CpIr(PH_3)(CH_3)^+$ (13 kcal/mol). Clearly, these calculational results strongly suggest that *the oxidative addition of the rhodium complex is intrinsically more difficult than that of the iridium complex*. We thus predict that the C−H bond activation by the $CpM(PH_3)(CH_3)^+$ complex will be inhibited when the central metal is rhodium.

3. The Origin of the Barrier and the Reaction Enthalpy for Oxidative Addition of $CpM(PH_3)(CH_3)^+$ (M = Rh and Ir). For better understanding the chemical reactivity and bonding nature of the 16-electron $CpM(PH_3)(CH_3)^+$ species, a simple valence bond model is used to develop an explanation for the barrier heights as well as the reaction enthalpy discussed above.

According to Su's study[20] based upon the configuration mixing (CM) model described by Pross and Shaik,[21] it was suggested that the singlet−triplet gap of carbene plays a crucial role in insertion reactions, i.e., the relative stabilities of the lowest singlet and triplet states are in turn a sensitive function of the barrier height for carbenic reactivity. Since, as already mentioned, 16-electron $CpM(PH_3)(CH_3)^+$ is isolobal to CH_2:,[7] one may envision that the predictions for carbenic reactivity should also apply to the former.

In principle, the oxidative addition reaction may exist in a number of predetermined states, each of which may be approximated by the appropriate molecular orbital configuration. Nevertheless, as shown schematically in Figure 9, there are only two predominant configurations that contribute considerably to

(20) Su, M.-D. *Inorg. Chem.* **1995**, *34*, 3829.
(21) (a) Shaik, S.; Schlegel, H. B.; Wolfe, S. *Theoretical Aspects of Physical Organic Chemistry*; John Wiley & Sons Inc.: New York, 1992. (b) Pross, A. *Theoretical and Physical principles of Organic Reactivity*; John Wiley & Sons Inc.: New York, 1995.

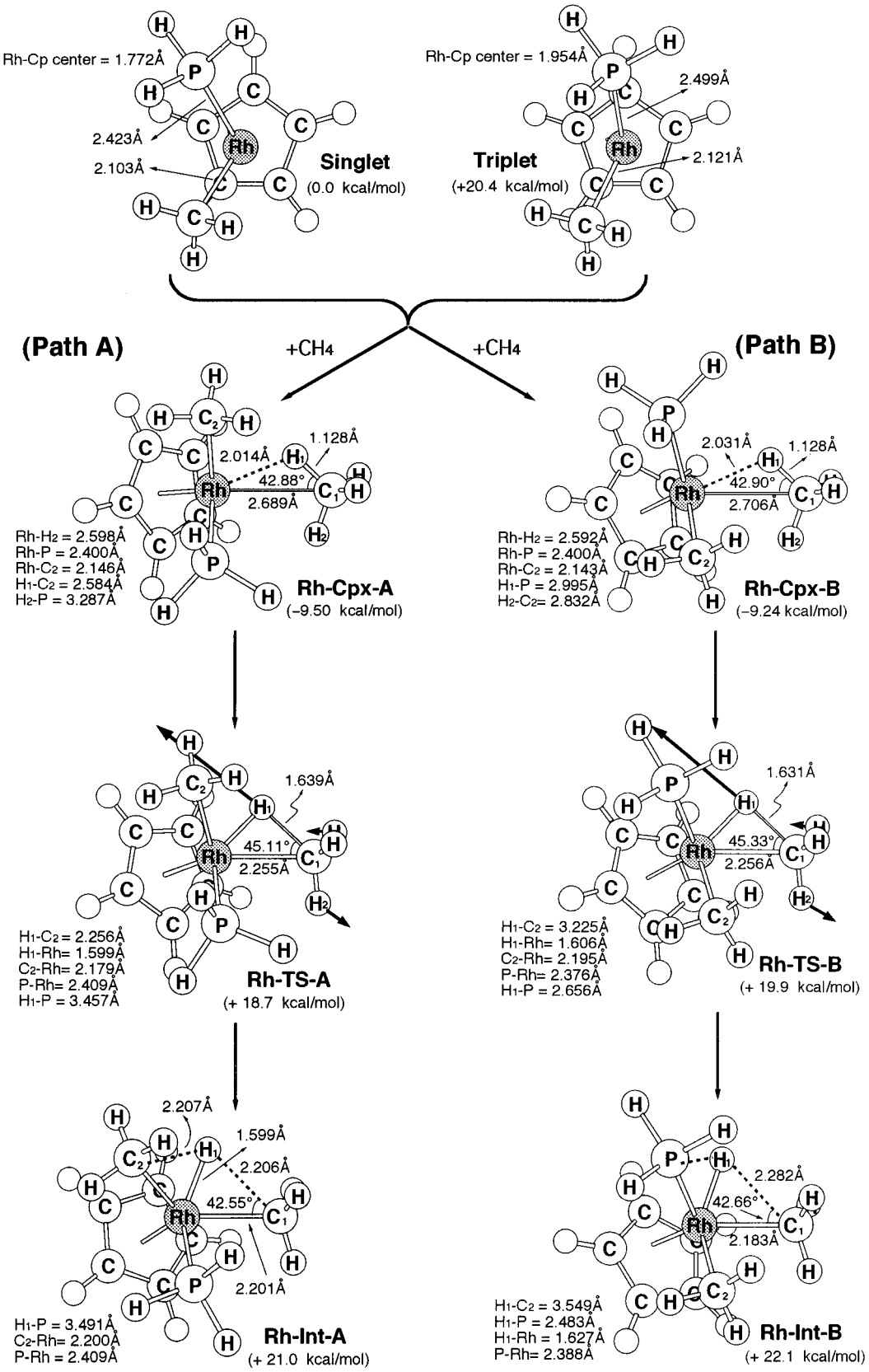

Figure 6. The MP2/LANL2DZ optimized geometries at reactants (singlet and triplet), agostic complexes (Cpx), transition states (TS), and intermediate (Int) of $CpRh(PH_3)(CH_3)^+$ for path A and path B. See the text for details. The values in parentheses are the relative energies at the QCISD//MP2/LANL2DZ level. The heavy arrows indicate transition vectors for the single imaginary frequency described by the transition states **Rh-TS-A** (-652 cm^{-1}) and **Rh-TS-B** (-691 cm^{-1}).

the total wave function Ψ and, in turn, affect the shape of the singlet surface. One is the reactant ground-state configuration ϕ_1 that ends up as an excited configuration in the product region. The other is the excited configuration of the reactants, ϕ_2, that correlates with the ground state of the products. There are, of course, other intermediate configurations with different spin states that might contribute to the total wave function Ψ. But since we are only concerned with singlet states in the course of

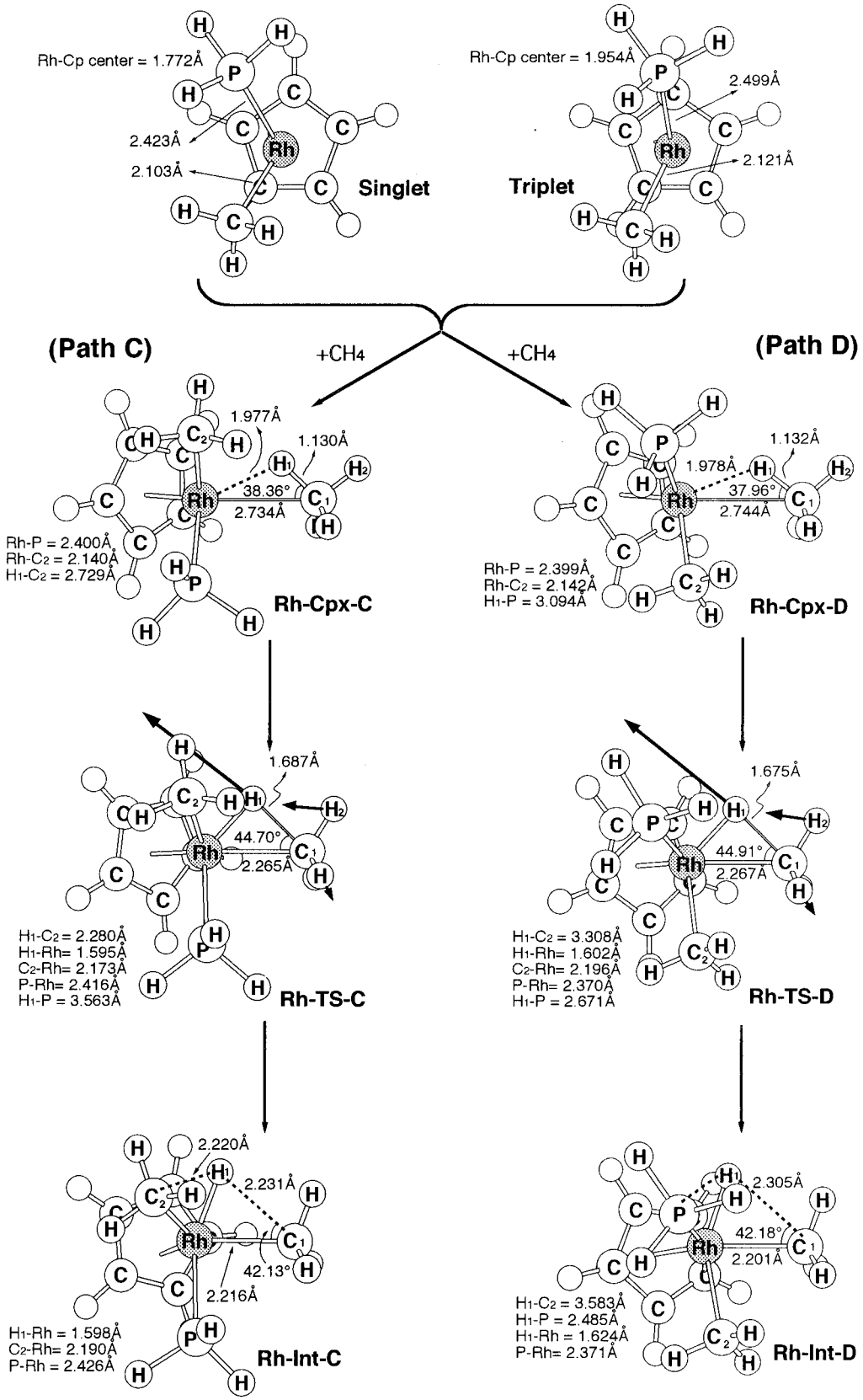

Figure 7. The MP2/LANL2DZ optimized geometries at reactants (singlet and triplet), agostic complexes (Cpx), transition states (TS), and intermediate (Int) of $CpRh(PH_3)(CH_3)^+$ for path C and path D. See the text for details. The heavy arrows indicate transition vectors for the single imaginary frequency described by the transition states **Rh-TS-C** (-600 cm^{-1}) and **Rh-TS-D** (-641 cm^{-1}).

reaction, it can be assumed that those intermediate configurations contribute very little, if at all, to Ψ and can therefore be neglected. In consequence, the reaction complex at any point on the reaction profile can be described by Ψ, a linear combination of ϕ_1 and ϕ_2, and the character of the transition state will reflect the extent of mixing between ϕ_1 and ϕ_2 in the region of the avoided crossing. Thus, it is the avoided crossing of these two configurations that leads to the simplest description of the ground state energy profiles for oxidative additions of 16-electron $CpML_2^+$. It is notable that the product configuration

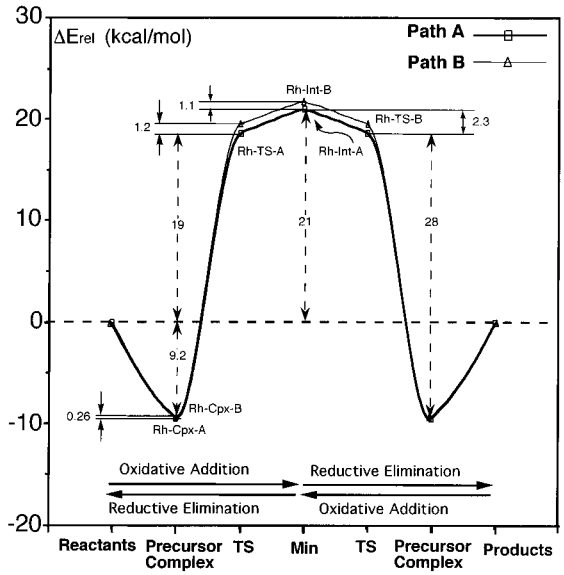

Figure 8. Potential energy surfaces for the activation of the methane C−H bond by $CpRh(PH_3)(CH_3)^+$. The relative energies are taken from the QCISD//MP2/LANL2DZ level as given in Table 1. The heavy solid curve indicates path A, while the solid curve indicates path B. For the MP2 optimized structures of the stationary points for paths A and B see Figure 6.

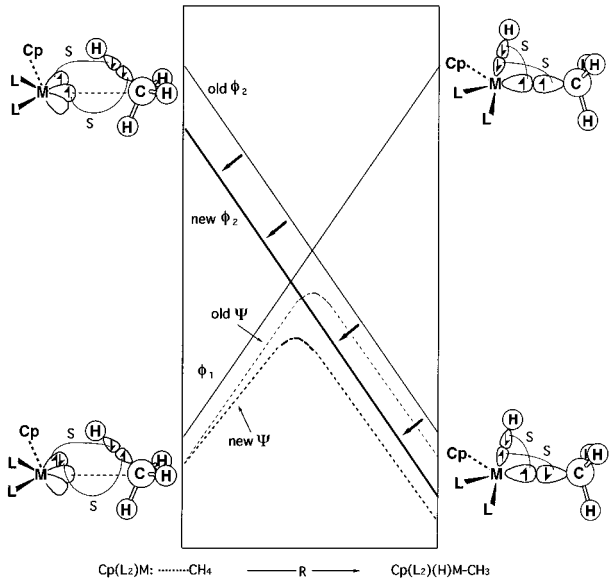

Figure 9. Energy diagram for an oxidative addition reaction showing the formation of a state curve (Ψ) by mixing two configurations: the reactant configuration (ϕ_1) and the product configuration (ϕ_2). S stands for singlet. This energy diagram also shows the effects of stabilizing the product configuration ϕ_2 (indicated by the heavy arrows).

ϕ_2 (doubly excited with respect to the reactant configuration ϕ_1) forms an overall singlet state and allows both M−H and M−C bond formation and simultaneous C−H′ bond breaking. Moreover, since the barrier height is basically governed by the avoided crossing of the configuration ϕ_1 and ϕ_2, it is apparent that a $\phi_1 \rightarrow \phi_2$ excitation will correlate with the barrier. Accordingly, if a factor is introduced into the system that has the effect of stabilizing ϕ_2, then ϕ_2 will be displaced to a lower energy along the entire reaction coordinate (see Figure 9, as indicated by the heavy arrows).[20,21] The effect of such a perturbation is predicted (i) to lower the reaction barrier since the intended crossing of ϕ_1 and ϕ_2 is lower in energy and (ii) to produce a larger exothermicity for the energy of product that is now lower than that of reactant.

From the above analysis, it is apparent that both ΔE_{st} ($=E_{triplet} - E_{singlet}$ for $CpML_2^+$) and $\Delta E_{\sigma\sigma^*}$ ($=E_{triplet} - E_{singlet}$ for CH_4) will determine the activation energy as well as the reaction enthalpy for such oxidative addition reactions. Therefore, if $\Delta E_{\sigma\sigma^*}$ is a constant, then a smaller value of ΔE_{st} results in a lower barrier height and a larger exothermicity. Indeed, from the valence-bond point of view (bottom right in Figure 9), the bonding in the product can be recognized as bonds formed between the triplet $CpML_2^+$ and the two doublet radicals (overall singlet), the methyl radical, and the hydrogen atom. This is much the same as viewing the bonding in the water molecule as bonds formed between the triplet oxygen atom and the two doublet hydrogen atoms. Thus, in order to form the strongest chemical bonds between $CpML_2^+$ and methane, it requires a singlet to triplet promotion energy for the $CpML_2^+$ fragment. In other words, *those oxidative addition reactions in which 16-electron $CpML_2^+$ complexes have large singlet−triplet gaps ($\Delta E_{st} = E_{triplet} - E_{singlet}$) will have larger barriers as well as smaller exothermicity than reactions whose corresponding complexes have small singlet−triplet gaps.* Our calculational results based on the MP2 and QCISD methods confirmed this prediction. For instance, as shown in Table 1, at the QCISD level singlet $CpIr(PH_3)(CH_3)^+$, which has a lower ΔE_{st} (16.6 kcal/mol), lies below the triplet, and ϕ_1 rises relatively little before it crosses ϕ_2, resulting in a smaller barrier (6.02 kcal/mol). On the other hand, singlet $CpRh(PH_3)(CH_3)^+$ is more stable than the triplet ($\Delta E_{st} = 20.4$ kcal/mol); thus, ϕ_1 must rise steeply and yields a higher barrier (18.7 kcal/mol) as a result of its crossing with ϕ_2.[22]

Furthermore, one may wonder, in the Rh and Ir systems, why $CpIr(PH_3)(CH_3)^+$ is a good model for a facile oxidative addition process. Considering the nature of the central metal, as discussed by Siegbahn,[23] since the energy required to change from a high spin ground state (quartet) to a low spin state (doublet) is much larger for the iridium atom (60.7 kcal/mol) than for the rhodium atom (7.8 kcal/mol), one may readily conclude that the iridium system would prefer to remain in the high spin state. This phenomenon would, in turn, cause the $CpIrL_2^+$ system to have a smaller ΔE_{st} ($=E_{triplet} - E_{singlet}$). Conversely, the excitation energy difference in going from the high spin state to the low spin state for the rhodium atom is so small that the singlet−triplet gap of the $CpRhL_2^+$ species should be larger than that of $CpIrL_2^+$. Consequently, *for the 16-electron $CpML_2^+$ cases the oxidative addition of a third-row transition metal (such as Ir), which can lead to a smaller ΔE_{st}, will be preferable to that of a second-row transition metal (such as Rh).* On the other hand, the ligand effect, which can modulate the electron density at the reacting metal center, will, of course, affect the singlet−triplet gap of the reactant so that it also plays a dominant role in the activation of C−H bonds of alkanes. The ligand effect and the nature of the central metal on this chemistry are currently being investigated along the series and will be given elsewhere.[24]

V. Conclusion

This work represents an attempt to apply the FMO model to predict the approximate reaction trajectory and transition state

(22) As shown in Figure 8, the fact that **Rh-Int-A** is an unstable intermediate and might become a transition state in contrast to the **Ir-Int-A** case reflects its less exothermicity for such oxidative addition reactions. Incidentally, the difference of the reaction enthalpy between the Ir and Rh cases is about 22 kcal/mol at the QCISD//MP2/LANL2DZ level, which compares with the value of about 30 kcal/mol for the CpML (M = Rh, Ir) + CH_4 systems at the B3LYP/LANL2DZ level. See: Su, M.-D.; Chu, S.-Y. Submitted for publication.

(23) Siegbahn, P. E. M. *J. Am. Chem. Soc.* **1996**, *118*, 1487.

(24) Su, M.-D.; Chu, S.-Y. Manuscript in preparation.

structures for the activation of saturated C−H bonds by 16-electron $CpM(PH_3)(CH_3)^+$ (M = Rh, Ir) and then to understand the origin of their barriers using the CM model as a qualitative tool. Despite the fact that the estimated magnitude of the barrier and the predicted geometry of the transition state for such reactions appear to be dependent on the calculational level applied, our qualitative predictions are in agreement with the calculational results presented here. Especially, our study has shown that the problems concerning the chemical reactivity of the 16-electron $CpML_2^+$ systems can be reduced to pictorial considerations. In spite of its simplicity, our approach proves to be rather effective and can provide chemists with important insights into the factors controlling the activation of saturated C−H bonds, thus allowing a better understanding of the nature of such systems as well as a number of predictions to be made. For instance, we predict the following:

(1) For the $CpIr(PH_3)(CH_3)^+$ species, path 1 (Scheme 1), which undergoes a reversible reaction involving an oxidative addition−reductive elimination process, is energetically feasible from both a kinetic and a thermodynamic viewpoint.

(2) For the 16-electron $CpML_2^+$ systems, a stronger electron-donating ligand (such as PMe_3) and a heavier transition metal center (i.e., the third row) will lead to a smaller ΔE_{st} and, in turn, will facilitate the activation of alkane C−H bonds.

(3) In contrast, for the 16-electron $CpML_2^+$ systems, a better electron-withdrawing ligand (such as CO) and a lighter transition metal center (i.e., the second-row) will result in a larger ΔE_{st} and then may hinder the activation of saturated C−H bonds.

We are eagerly awaiting further experimental evidence.

Acknowledgment. The authors thank the National Center for High-Performance Computing of Taiwan and the Computing Center at Tsing Hua University for generous amounts of computing time. In addition, they thank the National Science Council of Taiwan for financial support. They also thank Professor H. B. Schlegel for providing a useful software package and are grateful to referees for critical comments and helpful corrections of the manuscript.

Supporting Information Available: Listing of Cartesian coordinates for various MP2/LANL2DZ optimized structures (15 pages). See any current masthead page for ordering and Internet access instructions.

JA961847R